


Reversible microfluidic measurement with zinc tetraphenylporphyrin aiming at slipping NH₃ detection

Hao Zhou , Qi Yin, Zheng Yang, Yilin Song

State Key Laboratory of Clean Energy Utilization, Zhejiang University, Hangzhou, 310027, People's Republic of China

✉ E-mail: zhouhao@zju.edu.cn

Published in Micro & Nano Letters; Received on 27th February 2020; Revised on 11th June 2020; Accepted on 30th June 2020

A microfluidic chip that can realise reversible and highly selective NH₃ detection by separating NH₃ from the complex environment is fabricated for slipping NH₃ detection. The microfluidic chip consisting of the reaction unit, the gas-diffusion unit and detection unit applied the immobilised zinc tetraphenylporphyrin as the indicating material. The continuous spectrum change showed the light intensity decreased in the green range (500–550 nm). Based on the analysis of the spectrum change at 528 nm, a one-to-one relationship between the spectrum change and concentration was revealed. The reversibility of the detection process makes the detection advantageous. Also, the rapidity of the proposed method is proved by the time responses of the indicating and recovering processes. According to the 40 tests conducted for various concentrations, it was concluded that the results are stable and the entire system is reliable.

1. Introduction: Ammonia (NH₃) is a kind of colourless but pungent gas that has an enormous biological hazard, which causes permanent damage with a concentration of over 200 ppm. Meanwhile, ammonia is extremely soluble so that aquatic animals also suffer from its poisonousness. There are various sources of ammonia on earth [1]. Among these, the selective catalytic reduction (SCR) method where ammonia is injected into the SCR reactor to transform NO_x into N₂ is applied in many coal-fired power plants to reduce NO_x emission. Though the SCR method produces expectant results, it also brings new problems. Insufficient ammonia will reduce the SCR efficiency while excessive ammonia will result in the unreacted ammonia going into the downstream flue, which is called ammonia slipping. Part of the slipping ammonia would react with the SO₃ derived from the combustion process of coal and form sulfates [2] and the other part would be emitted into the air. NH₄HSO₄ (ABS) is one of the most harmful sulfates because it would cause the issues of blocking and etching in the SCR reactor [3]. So the detection of slipping ammonia is of great significance. It can not only help to maintain a high-denitration efficiency but also avoid blocking and etching of the flue or emission of ammonia into the atmosphere.

Currently, effective ammonia detection methods are mainly divided into laser-based methods [4] and spectrophotometric methods [5, 6]. The laser-based methods, such as near-infrared diode-laser spectroscopy [7], tunable diode laser absorption spectroscopy [8, 9] and Fourier transform infrared spectrometer [10, 11] tend to measure the absorption of the laser with a specific wavelength to obtain the ammonia concentration. The laser-based methods are suitable for online ammonia measurement. However, there are still some problems that need to be solved, like the shaking of the boiler and the excessive fly ash blocking the laser.

The spectrophotometric methods measure the colour change with a spectrophotometer during the reaction of ammonia and dye to determine the ammonia concentration [12]. The famed Berthelot method based on phenol and hypochlorite has been used as a standard means in previous research [13]. The spectrophotometric methods usually have two steps: sampling and analysis. The sampling step extracts a certain amount of gas and pumps it into the acid absorption solution (H₂SO₄) so that ammonia is converted into ammonium ions. The analysis step mixes the indicator material and the absorption solution, followed by spectrophotometric measurement. These methods for ammonia measurement are accurate and stable. However, they have many common disadvantages

including the non-reutilisation of the absorption solution, the complex and prolonged operation and the susceptibility to interference.

Microfluidics has attracted great attention in biological, chemical and optical areas since the 1990s [14] due to its rapid and precise ability of analysis. Microfluidics has been also applied to the area of ammonia detection [15–18]. Compared with the macro spectrophotometric methods mentioned above, the spectrophotometric measurement in microfluidics is rapid, efficient and integrated. In fact, the Berthelot method has already been introduced into microfluidic chips to measure ammonia concentration [19]. Besides, salicylate [20], oxazine [21], bromophenol blue [22], phenol red [23], rhodamines [24] and porphyrins have all been used as the indicating materials. Among them, porphyrin-based materials (compounds) have been proved to be suitable indicators in chemical sensing of various kinds of pollutants [25], including NO₂ [26], H₂O₂ [27] and Hg²⁺ [28]. Zinc tetraphenylporphyrin (ZnTPP) is superior in ammonia sensing as a natural chromophore with high reversibility. Early reports intended to integrate ZnTPP with films [29, 30], but the short service life and low utilisation ratio restricted its application. Inlaying ZnTPP into microfluidic chips has now been a primary trend and has made great progress [31, 32]. However, ZnTPP cannot be used for ammonia detection in a complex environment due to its poor selectivity. Therefore, in the sampling analysis of flue gas, the direct measurement of ammonia is still very challenging with the low concentration and complex composition of the flue gas. Further research needs to be done to settle this problem.

In this work, a microfluidic chip that applied ZnTPP-dyed cation exchange resin microbeads as the indicating material was fabricated for reversible slipping ammonia measurement. Highly selective ammonia detection in complex solution was realised by the integrated experimental system. The spectrum was analysed to obtain the intensity change for various wavelengths. The data for different ammonia concentrations at 528 nm were selected for further investigation. The spectrum intensity change of the indicating process and the recovering process demonstrated the reversible detection characteristic and rapid response. The results of experiments for each ammonia concentration confirmed the stability of the system.

To the knowledge of the authors, most of the existing microfluidic ammonia detection devices were paper-based [33, 34] and often used in medical diagnosis [33, 35]. These devices were mostly designed to be disposable. By contrast, our device is reusable,

which makes it more beneficial to save the cost in the industry. Besides, a complex micro-distillation technique [36] or even no technique [37] was used to selectively separate ammonia in previous work. Compared with them, we used a polydimethylsiloxane (PDMS) membrane to achieve efficient ammonia separation, which was extremely easy to operate.

2. Experimental setup

2.1. Preparation of ZnTPP and solution: The cation exchange resin microbeads (Dowex 50WX4 hydrogen form, J&K) were filtrated for those with a diameter of 50–60 μm . In total, 30 mg of ZnTPP (5, 10, 15, 20-tetraphenyl-21H, 23H-porphine zinc, J&K) was first dissolved in ethanol solution composed of 1.5 ml of ethanol and 5 ml of deionised water. In total, 650 mg of cation exchange resin microbeads were then mixed with 6.5 ml of deionised water to form a mixture into which the ZnTPP solution was added. A magnetic stirrer was used to stir the entire mixture for 10 h. The redundant ZnTPP was filtered off by washing the ZnTPP-dyed microbeads with ethanol constantly until the ethanol was thoroughly transparent. After that, the dyed microbeads (green) were dried for 5 h.

We used $(\text{NH}_4)_2\text{SO}_4$ (J&K) and deionised water to prepare a solution with corresponding concentrations. The solution was prepared according to the weight of NH_4^+ and all the concentrations were referred with respect to NH_4^+ concentrations. NaOH (Sinopharm Chemical Reagent Co., Ltd.), ethylene diamine tetraacetic acid (EDTA) and deionised water were used to prepare NaOH solution (NaOH: 1M, EDTA: 0.1M).

2.2. Fabrication of the microfluidic chip: The microfluidic chip that is shown in Fig. 1 consisted of three independent units: the reaction unit, the gas-diffusion unit and the detection unit. Each unit was fabricated separately since they were made with different techniques.

The reaction unit was composed of two layers. The upper layer was made of PDMS (DC-184, Dow Corning) which contained the reaction channel (width: 100 μm and depth: 100 μm). The

details can be seen in our previous work [38]. The bottom layer (a piece of glass) was bonded with the upper layer with plasma treatment to form covalent bonds. The reaction unit contained two inlets, one outlet and the channels. $(\text{NH}_4)_2\text{SO}_4$ solution and NaOH solution were injected into the channel from two inlets, respectively. Solution streaming out of the outlet became the donor solution.

The gas-diffusion unit contained three layers: the upper glass layer that contained the upper channel, the middle gas-diffusion membrane layer, and the bottom glass layer that contained the bottom channel. The process of the fabrication of the upper and bottom glass layers can be seen in previous work [39]. Each glass layer had one inlet and one outlet. The upper channel and the bottom channel were with the same shape but the inlets and outlets were staggered. PDMS was selected as the material of the middle gas-diffusion membrane layer for its hydrophobicity and gas permeability. So a piece of PDMS membrane (thickness: 10 μm) was placed in the middle and bonded with the upper and bottom glass layers with plasma treatment. The inlet of the bottom glass layer was connected to the outlet of the reaction unit with a polytetrafluoroethylene (PTFE) tube. The acceptor solution (deionised water) was injected into the gas-diffusion unit from the inlet of the upper glass layer. As the donor solution flowed through the bottom channel, NH_3 would diffuse from the donor solution to the acceptor solution through the gas-diffusion membrane with no exchange of liquid components. The outlet of the upper glass layer was connected to the inlet of the detection unit by a PTFE tube while the solution that came out of the bottom glass layer became waste.

The detection unit applied a four-layered structure: glass–PDMS–glass–PDMS (from bottom to top). The bottom glass was used as the substrate on which a thin layer of PDMS (liquid) was coated. Another piece of glass with a 10-mm penetrated hole was placed on the PDMS layer and 5 mg of ZnTPP dyed cation exchange resin microbeads were cast onto the PDMS layer through the hole. The three-layer structure was then heated at 80°C and the PDMS layer became solidified and bonded with two glass layers. The top PDMS layer was made in the same way as the reaction unit and had one inlet and one outlet. The three-layered structure was bonded permanently with the top PDMS layer by plasma treatment to form a four-layered integrated chip. The penetrated hole cast with ZnTPP dyed cation exchange resin microbeads was the detection area of the detection unit. The acceptor solution, which contained NH_3 flowed through the detection unit and caused the colour change of ZnTPP. The solution flowing out of the outlet became waste and was technically treated.

2.3. Integrated system: The integrated experimental system is also shown in Fig. 1. An LED light was used as the light source. A collimator was placed above the LED light to form a beam of parallel light. Then the light passing upright through the detection area of the detection unit was then collected by a convex lens. The focused light after the convex lens went into the optical fibre. The results were analysed by the portable spectrophotometer (USB 650, Ocean Optics) and the data were recorded by a personal computer. Three syringe pumps (Elite Pump 11, Harvard) were used to inject various reagents into the microfluidic chips.

3. Results and discussion

3.1. Detection principle: The detection principle can be explained on the basis of Lewis theory of acid–base reactions. Metalloporphyrins are expected to be sensitive to Lewis bases that can donate their lone electron pairs to the metalloporphyrin metal ions that behave as Lewis acids [31]. The detection is based on the fact that ZnTPP can accept the lone pair electrons of the NH_3 molecule. During the reaction, ZnTPP turns from green to purple, causing the spectrum change and this process is called the indicating process. When pure water is around, ZnTPP will be

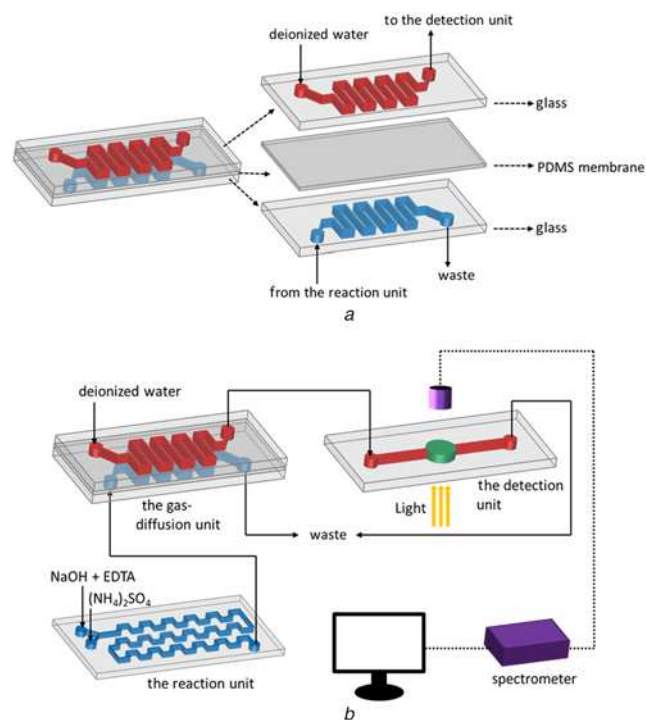


Fig. 1 Schematic representations of
a Gas-diffusion unit
b Integrated system

separated from the NH_3 molecules and turn from purple back to green. This process is called the recovering process.

The complex flue gas contained N_2 , O_2 , CO_2 , H_2O , SO_2 (SO_3), NO_x , NH_3 , HCl , HF . Being the only alkaline component, NH_3 was converted into NH_4^+ after being absorbed by a sufficient quantity of H_2SO_4 . It is impossible to conduct direct detection in complex solution because ZnTPP can only react with NH_3 instead of NH_4^+ . Furthermore, NO_x can also make ZnTPP change colour [26] and introduce interference. So NaOH was applied to adjust the absorbent to alkaline. Under a high pH, NH_4^+ was converted into NH_3 which diffused into the acceptor solution through the gas-diffusion membrane while other components remained unchanged. NH_3 was separated from the complex environment through the reaction unit and the gas-diffusion unit. The reason why deionised water was selected as the acceptor solution rather than NaOH was that NaOH can also react with ZnTPP and make it purple [31]. The gas-diffusion membrane also avoided the interference of NaOH by preventing it from going into the acceptor solution from the donor solution. Pre-experiments were conducted in which NaOH solution was injected into the gas-diffusion unit. The results showed that no spectrum change was observed. This confirms that the interferences in the complex environment will not affect NH_3 detection. In fact, amines that did not exist in the flue gas are the only compounds that can interfere with the detection.

3.2. Highly selective detection performance: Spectrum data were collected every 10 s with the integration time being 8 ms. The detection wavelength ranged between 200 and 800 nm. Before experiments, the dark spectrum is recorded and then it was subtracted in the subsequent spectrums. All spectrums were normalised to its max intensity. Deionised water was first injected into the detection unit to obtain the reference spectrum. The reference spectrum normalised to max intensity was recorded as S_{ref} . Then NH_4^+ solution of various concentrations and NaOH solution were both injected into the reaction unit at the flow rate of 1 $\mu\text{L}/\text{min}$. The acceptor solution (deionised water) was injected into the gas-diffusion unit at the flow rate of 2 $\mu\text{L}/\text{min}$. The obtained measurement spectrums were normalised and recorded as S_{mea} . All the solution was constantly injected until the spectrum was stable. After that, all the solution was changed into deionised water until the recovering process was over and the spectrum became stable again.

The spectrum intensity change ΔS is defined by the following equation:

$$\Delta S = S_{\text{mea}} - S_{\text{ref}} \quad (1)$$

$\Delta S > 0$ means spectrum intensity increases and $\Delta S < 0$ means spectrum intensity decreases, $\Delta S = 0$ means a same intensity.

Fig. 2 shows the continuous ΔS of the indicating process for NH_4^+ concentration of 5 mg L^{-1} . It is obvious that spectrum intensity

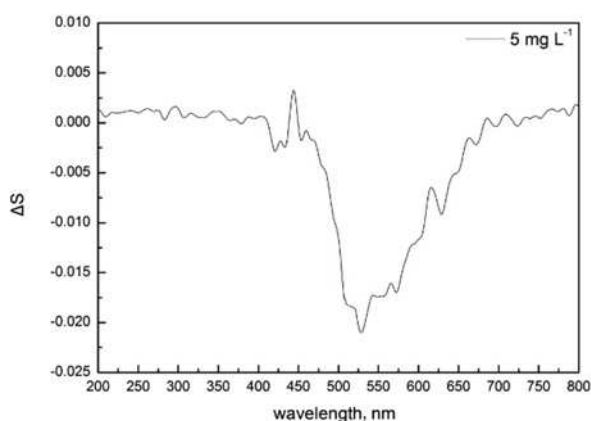


Fig. 2 Continuous ΔS of the indicating process for NH_4^+ concentration of 5 mg L^{-1}

decreased in the range of 500–550 nm, which belongs to green light. It was attributed to ZnTPP turning from green to purple after the reaction with NH_3 . ΔS reached a peak at the wavelength of 528 nm and the value was about -0.021 . When NH_4^+ concentration was changed, curves with similar shape but different amplitudes were obtained. This trend illustrates that ΔS can be used to directly indicate the NH_3 (NH_4^+) concentration in a complex environment.

For further investigation, we extracted ΔS at 528 nm under various NH_4^+ concentration. Each result was the average of five tests. All the results were converted into absolute values as shown in Fig. 3.

It is clear that ΔS increased significantly with the rising NH_4^+ concentration. The value was merely 0.018 with the NH_4^+ concentration of 1 mg L^{-1} , but it rose to 0.048 for 25 mg L^{-1} . Various concentrations could be easily distinguished. It makes sense that the rising rate became higher when NH_4^+ concentration was comparably high ($> 5 \text{ mg L}^{-1}$). ΔS at 528 nm formed a one-to-one relationship with the NH_4^+ concentration, which can be used to realise sampling analysis of NH_3 slipping. Limit of detection (LOD) refers to the corresponding amount of three times of instrument background signal generated by matrix blank. The LOD of our device was 0.1 mg L^{-1} .

3.3. Reversibility and time response: The change of ΔS versus time at 528 nm for NH_4^+ concentration of 5 mg L^{-1} is shown in Fig. 4. From 0 to 5.5 min, ΔS increased rapidly with time, which meant that the indicating process happened mainly in this period. ΔS reached 0.192 at 5.5 min. From 5.5 to 6.5 min, ΔS increased

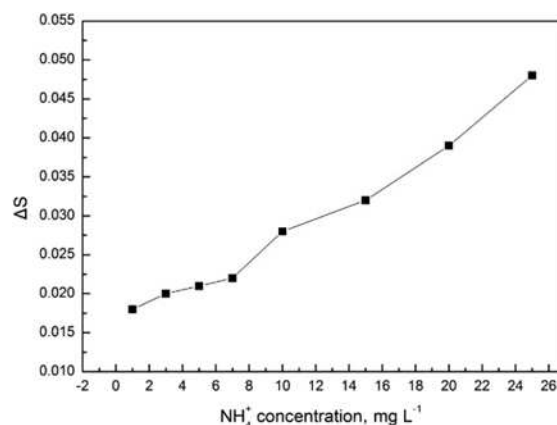


Fig. 3 ΔS at 528 nm for various NH_4^+ concentrations

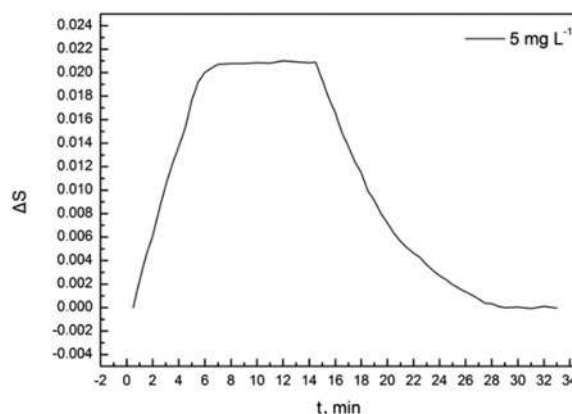


Fig. 4 Change of ΔS versus time at 528 nm for NH_4^+ concentration of 5 mg L^{-1}

slowly to about 0.21 and became steady with some negligible fluctuations after 6.5 min. It was concluded that the time for indicating process was about 6.5 min. ΔS began to decrease at 15 min and the recovering process started. Similarly, to the indicating process, ΔS varied fast and then slowly. Finally, ΔS turned back to 0 at 26.9 min with some negligible fluctuations. The time for the recovering process was about 11.9 min. The indicating process and the recovering process confirm the reversibility of the reaction between ZnTPP and NH_3 . The fact that ΔS turned back to 0 proved that ZnTPP regressed thoroughly to the original state. Compared with the indicating materials that can not be used repeatedly, the reversibility of ZnTPP is superior undoubtedly. It means that indicating materials can be recycled and the costs can be reduced. Besides, ZnTPP was immobilised in the microfluidic chip firmly to avoid repetitive preparation, which makes the detection operation simple. The time for the indicating process and the recovering process was found to be constant through five times of tests under the same concentration.

Then the time of the indicating process and the recovering process for various NH_4^+ concentrations was tested. We found that the time for both processes changed with NH_4^+ concentration. Each result was the average of five tests and they are exhibited in Fig. 5. It was concluded that the time of the indicating process and the recovering process both increased corresponding with the rising NH_4^+ concentration, but the increasing trend of the recovering process was more significant than that of the indicating process. Even under the NH_4^+ concentration of 25 mg L^{-1} , the recovering time was only 14.4 min, which was indeed very fast. The time for the indicating process and the recovering process was constant for a certain NH_4^+ concentration, which means we can estimate the needed detection time. For ammonia slipping detection, 7.7 min is adequate for the indicating process and 14.4 min for the recovering process. The recovering process always needed more time than the indicating process. This phenomenon might be attributed to the reason that the decomposition of the resultant is more difficult than the incorporation of ZnTPP and NH_3 . ΔS became 0 after the recovering process on all accounts and ZnTPP was used 40 times without obvious degradation.

3.4. Stability: We conducted five tests for each of the eight concentrations as mentioned above. All the results of the indicating process are shown in Fig. 6. It is obvious that the results were stable for each concentration. Even for low NH_4^+ concentrations ($1, 3, 5, 7 \text{ mg L}^{-1}$), each result under a certain concentration was significantly distinguished from that under another concentration. The relative standard deviations were 2.4, 1.7, 2.2, 1.2, 1.4, 0.7, 0.9 and 0.7%, respectively, in order of NH_4^+ concentration from low to high. It can be concluded that the fluctuation ranges for all the

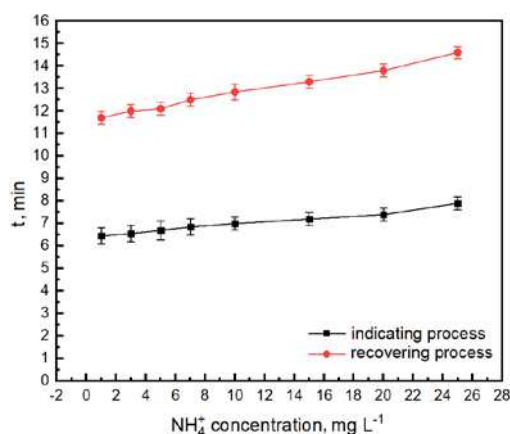


Fig. 5 Time of indicating process and recovering process for various NH_4^+ concentrations

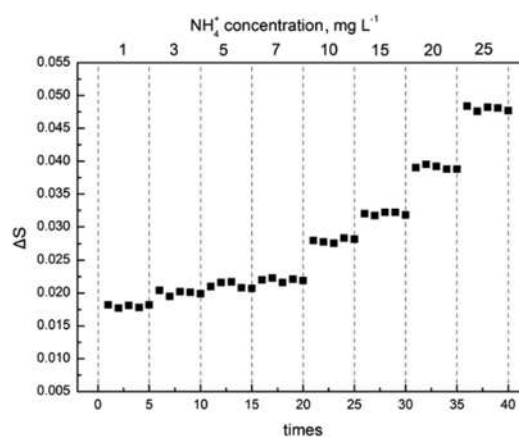


Fig. 6 Stability test for various NH_4^+ concentrations

tested NH_4^+ concentrations were almost the same. The results demonstrate a high stability of the detection method for various NH_4^+ concentrations.

There might be some elements, in the microfluidic chip, that could affect the ammonia detection like the mechanical strength and service life of the gas-diffusion membrane, the performance of ZnTPP and the immobilisation of the cation exchange resin microbeads. Fortunately, the stable results demonstrated that all the elements worked normally without any degeneration or damage.

4. Conclusion: To realise highly selective NH_3 detection in a complex environment and measure slipping ammonia coming from the SCR denitration process, a microfluidic chip was fabricated into which ZnTPP dyed cation exchange resin microbeads were embedded as the indicating material. An integrated system consisting of the reaction unit, the gas-diffusion unit and the detection unit was set up to separate NH_3 from the complex environment and realise reversible detection. The continuous spectrum intensity change, ΔS , showed that the light intensity in the green range (500–550 nm) decreased due to the colour change of ZnTPP after reacting with NH_4^+ of various concentrations. ΔS at 528 nm exhibited good performance in NH_4^+ detection. The value was merely 0.018 when NH_4^+ concentration was 1 mg L^{-1} , but it rose to 0.048 for 25 mg L^{-1} . The one-to-one relationship was particularly recognisable under high concentrations of NH_4^+ . Good reversibility can be confirmed through the relationship between ΔS and time at 528 nm. It helps to save indicating materials, reduce costs and simplify operation. The time of the indicating process and the recovering process both increased with the rising NH_4^+ concentration, but the recovering process always needed a longer time than the indicating process. 7.7 min was adequate for the indicating process while 14.4 min for the recovering process. Finally, based on the analysis of all the 40 tests for eight various NH_4^+ concentrations, the stability of the detection is confirmed. The calculated relative standard deviations were 2.4, 1.7, 2.2, 1.2, 1.4, 0.7, 0.9 and 0.7%, respectively in order of NH_4^+ concentration from low to high. The introduced system can stably realise reversible and highly selective NH_3 detection in a complex environment.

5. Acknowledgment: This work was supported by the National Science Fund for Distinguished Young Scholars (No.51825605).

6 References

- [1] Timmer B., Olthuis W., Berg A.V.: 'Ammonia sensors and their applications—a review', *Sens. Actuators B, Chem.*, 2005, **107**, (2), pp. 666–677
- [2] Shi Y., Shu H., Zhang Y., ET AL.: 'Formation and decomposition of NH_4HSO_4 during selective catalytic reduction of NO with NH_3

- over V_2O_5 - WO_3 /TiO₂ catalysts', *Fuel Process. Technol.*, 2016, **150**, pp. 141–147
- [3] Muzio L., Bogseth S., Himes R., *ET AL.*: 'Ammonium bisulfate formation and reduced load SCR operation', *Fuel*, 2017, **206**, pp. 180–189
 - [4] Deguchi Y., Kamimoto T., Kiyota Y.: 'Time resolved 2D concentration and temperature measurement using CT tunable laser absorption spectroscopy', *Flow Meas. Instrum.*, 2015, **46**, pp. 312–318
 - [5] Frank C., Schroeder F., Ebinghaus R., *ET AL.*: 'A fast sequential injection analysis system for the simultaneous determination of ammonia and phosphate', *Microchim. Acta*, 2006, **154**, (1–2), pp. 31–38
 - [6] El-Shahat M.F., Abdel-Halim S.H., El-Din M.A.: 'Micro determination of ammonia by a kinetic spectrophotometric method', *Microchim. Acta*, 2002, **140**, (1), pp. 51–54
 - [7] Claps R., Englich F.V., Leleux D.P., *ET AL.*: 'Ammonia detection by use of near-infrared diode-laser-based overtone spectroscopy', *Appl. Opt.*, 2001, **40**, (24), pp. 4387–4394
 - [8] Stritzke F., Diemel O., Wagner S.: 'TDLAS-based NH₃ mole fraction measurement for exhaust diagnostics during selective catalytic reduction using a fiber-coupled 2.2- μ m DFB diode laser', *Appl. Phys. B*, 2015, **119**, (1), pp. 143–152
 - [9] Peng Z., Ding Y., Lu C., *ET AL.*: 'Calibration-free wavelength modulated TDLAS under high absorbance conditions', *Opt. Express*, 2011, **19**, (23), pp. 23104–23110
 - [10] Sjövall H., Olsson L., Fridell E., *ET AL.*: 'Selective catalytic reduction of NO_x with NH₃ over Cu-ZSM-5 — the effect of changing the gas composition', *Appl. Catal. B, Environ.*, 2006, **64**, pp. 180–188
 - [11] Chen H., Wei Z., Kollar M., *ET AL.*: 'A comparative study of N₂O formation during the selective catalytic reduction of NO_x with NH₃ on zeolite supported Cu catalysts', *J. Catal.*, 2015, **329**, pp. 490–498
 - [12] Barczak M., McDonagh C., Wencel D.: 'Micro- and nanostructured sol-gel-based materials for optical chemical sensing (2005–2015)', *Microchim. Acta*, 2016, **183**, (7), pp. 2085–2109
 - [13] Zhu Z., Lu J.J., Almeida M.I., *ET AL.*: 'A microfabricated electro-osmotic pump coupled to a gas-diffusion microchip for flow injection analysis of ammonia', *Microchim. Acta*, 2015, **182**, (5–6), pp. 1063–1070
 - [14] Manz A., Graber N., Widmer H.M.: 'Miniaturized total chemical analysis systems: a novel concept for chemical sensing', *Sens. Actuators B, Chem.*, 1990, **1**, pp. 244–248
 - [15] Timmer B.H., van Delft M., Koelmans W.W., *ET AL.*: 'Selective low concentration ammonia sensing in a microfluidic lab-on-a-chip', *IEEE Sens. J.*, 2006, **6**, (3), pp. 829–835
 - [16] Evans G.P., Buckley D.J., Skipper N.T., *ET AL.*: 'Single-walled carbon nanotube composite inks for printed gas sensors: enhanced detection of NO₂, NH₃, EtOH and acetone', *RSC Adv.*, 2014, **4**, (93), pp. 51395–51403
 - [17] Chiang T.Y., Lin C.H.: 'A microfluidic chip for ammonium sensing incorporating ion-selective membranes formed by surface tension forces', *RSC Adv.*, 2014, **4**, pp. 379–385
 - [18] Martini-Laithier V., Graur I., Bernardini S., *ET AL.*: 'Ammonia detection by a novel Pyrex microsystem based on thermal creep phenomenon', *Sens. Actuators B, Chem.*, 2014, **192**, pp. 714–719
 - [19] Daridon A., Sequeira M., Pennarum-Thomas G., *ET AL.*: 'Chemical sensing using an integrated microfluidic system based on the Berthelot reaction', *Sens. Actuators B, Chem.*, 2001, **76**, pp. 235–243
 - [20] Hwang H., Kim Y., Cho J., *ET AL.*: 'Lab-on-a-disc for simultaneous determination of nutrients in water', *Anal. Chem.*, 2013, **85**, (5), pp. 2954–2960
 - [21] Jalal A.H., Yu J., Nnanna A.G.: 'Fabrication and calibration of oxazine-based optic fiber sensor for detection of ammonia in water', *Appl. Opt.*, 2012, **51**, (17), pp. 3768–3775
 - [22] Schmitt K., Rist J., Peter C., *ET AL.*: 'Low-cost fiber-optic waveguide sensor for the colorimetric detection of ammonia', *Microsyst. Technol.*, 2012, **18**, (7–8), pp. 843–848
 - [23] Mader H.S., Wolfbeis O.S.: 'Optical ammonia sensor based on upconverting luminescent nanoparticles', *Anal. Chem.*, 2010, **82**, (12), pp. 5002–5004
 - [24] Preininger C., Mohr G.J., Klimant I., *ET AL.*: 'Ammonia fluorosensors based on reversible lactonization of polymer-entrapped rhodamine dyes, and the effects of plasticizers', *Anal. Chim. Acta*, 1996, **334**, (1), pp. 113–123
 - [25] Paolesse R., Nardis S., Monti D., *ET AL.*: 'Porphyrinoids for chemical sensor applications', *Chem. Rev.*, 2016, **117**, (4), pp. 2517–2583
 - [26] Roales J., Pedrosa J., Guillén M., *ET AL.*: 'Free-base carboxyphenyl porphyrin films using a TiO₂ columnar matrix: characterization and application as NO₂ sensors', *Sensors*, 2015, **15**, (5), pp. 11118–11132
 - [27] Li X.R., Wang B., Xu J.J., *ET AL.*: 'Noncovalent assembly of picket-fence porphyrin on carbon nanotubes as effective peroxidase-like catalysts for detection of hydrogen peroxide in beverages', *Electroanalysis*, 2011, **23**, (12), pp. 2955–2963
 - [28] Liu X., Liu X., Tao M., *ET AL.*: 'A highly selective and sensitive recyclable colorimetric Hg²⁺ sensor based on the porphyrin-functionalized polyacrylonitrile fiber', *J. Mater. Chem. A*, 2015, **3**, (25), pp. 13254–13262
 - [29] Vaughan A.A., Baron M.G., Narayanaswamy R.: 'Optical ammonia sensing films based on an immobilized metalloporphyrin', *Anal. Commun.*, 1996, **33**, (11), pp. 393–396
 - [30] Nwachukwu F.A., Baron M.G.: 'Polymeric matrices for immobilising zinc tetraphenylporphyrin in absorbance based gas sensors', *Sens. Actuators B, Chem.*, 2003, **90**, (1–3), pp. 276–285
 - [31] Zilberman Y., Chen Y., Sonkusale S.R.: 'Dissolved ammonia sensing in complex mixtures using metalloporphyrin-based optoelectronic sensor and spectroscopic detection', *Sens. Actuators B, Chem.*, 2014, **202**, pp. 976–983
 - [32] Zilberman Y., Sonkusale S.R.: 'Microfluidic optoelectronic sensor for salivary diagnostics of stomach cancer', *Biosens. Bioelectron.*, 2015, **67**, pp. 465–471
 - [33] Thepchuay Y., Mesquita R.B.R., Nacapricha D., *ET AL.*: 'Micro-PAD card for measuring total ammonia nitrogen in saliva', *Anal. Bioanal. Chem.*, 2020, **412**, (13), pp. 3167–3176
 - [34] Peters J.J., Almeida M.I.G.S., O'Connor Sraj L., *ET AL.*: 'Development of a micro-distillation microfluidic paper-based analytical device as a screening tool for total ammonia monitoring in freshwaters', *Anal. Chim. Acta*, 2019, **1079**, pp. 120–128
 - [35] Kim S.B., Koo J., Yoon J., *ET AL.*: 'Soft, skin-interfaced microfluidic systems with integrated enzymatic assays for measuring the concentration of ammonia and ethanol in sweat', *Lab Chip*, 2020, **20**, (1), pp. 84–92
 - [36] Huang J., Chow C.W.K., Kuntke P., *ET AL.*: 'The development and evaluation of a microstill with conductance detection for low level ammonia monitoring in chloraminated water', *Talanta*, 2019, **200**, pp. 256–262
 - [37] Cai D., Tong T., Zhang Z., *ET AL.*: 'Functional film coated optical micro/nanofibers for high-performance gas sensing', *IEEE Sens. J.*, 2019, **19**, (20), pp. 9229–9234
 - [38] Zhou H., Yang Z., Yao Z., *ET AL.*: 'Application of digital holographic microscopy and microfluidic chips to the measurement of particle size distribution of fly ash after a wet electrostatic precipitator', *Flow Meas. Instrum.*, 2018, **60**, pp. 24–29
 - [39] Song Y., Shi Y., Li X., *ET AL.*: 'Afi-chip: an equipment-free, low-cost, and universal binding ligand affinity evaluation platform', *Anal. Chem.*, 2016, **88**, (16), pp. 8294–8301